Title Developmental hearing loss-induced perceptual deficits are rescued by cortical expression of $GABA_B$ receptors

Running Title $GABA_B$ expression restores perception

Authors Samer Masri[1], Regan Fair[1], Todd M. Mowery[5], Dan H. Sanes[1,2,3,4]

Addresses
[1] Center for Neural Science, New York University, 4 Washington Place, New York, NY 10003
[2] Department of Psychology, New York University
[3] Department of Biology, New York University
[4] Neuroscience Institute, New York University Langone Medical Center
[5] Brain Health Institute & Department of Otolaryngology, Rutgers University

Contact
Samer Masri, Ph.D.
Center for Neural Science
New York University
4 Washington Place
New York, NY 10003
Email sm9629@nyu.edu

Pages 20
Figures 4
Tables 0
Suppl Figs 2

Key Words
hearing loss, auditory cortex, auditory perception, synaptic inhibition, $GABA_A$, $GABA_B$

Abbreviations
auditory cortex (AC), gamma-aminobutyric acid A receptor subunit α1 (*Gabra1*), gamma-aminobutyric acid B receptor subunit 1b (*Gabbr1b*), hearing loss (HL), inhibitory postsynaptic potential (IPSP), amplitude modulation (AM), spectral modulation (SM).

Acknowledgements
The work is supported by NIDCD R01DC011284 (DHS and TMM), and F32DC020659 (SM).

Author Contributions
SM, TMM, and DHS designed the experiments and wrote the paper; SM, RF, and TMM performed experiments; SM and DHS designed the viruses.

Conflict of interest
The authors whose names are listed immediately above certify that they have no affiliations with or involvement in any organization or entity with any financial, or non-financial interest in the subject matter or materials discussed in this manuscript.

Abstract

Even transient periods of developmental hearing loss during the developmental critical period have been linked to long-lasting deficits in auditory perception, including temporal and spectral processing, which correlate with speech perception and educational attainment. In gerbils, hearing loss-induced perceptual deficits are correlated with a reduction of both ionotropic $GABA_A$ and metabotropic $GABA_B$ receptor-mediated synaptic inhibition in auditory cortex, but most research on critical period plasticity has focused on $GABA_A$ receptors. We developed viral vectors to express both endogenous $GABA_A$ or $GABA_B$ receptor subunits in auditory cortex and tested their capacity to restore perception of temporal and spectral auditory cues following critical period hearing loss in the Mongolian gerbil. HL significantly impaired perception of both temporal and spectral auditory cues. While both vectors similarly increased IPSCs in auditory cortex, only overexpression of $GABA_B$ receptors improved perceptual thresholds after HL to be similar to those of animals without developmental hearing loss. These findings identify the $GABA_B$ receptor as an important regulator of sensory perception in cortex and point to potential therapeutic targets for developmental sensory disorders.

Significance Statement

Hearing loss in children can induce deficits in aural communication that persevere even after audibility has returned to normal, suggesting permanent changes to the auditory central nervous system. In fact, a reduction in cortical synaptic inhibition has been implicated in a broad range of developmental disorders, including hearing loss. Here, we tested the hypothesis that developmental hearing loss-induced perceptual impairments in gerbils are caused by a permanent reduction of auditory cortical inhibitory synapse strength. We found that virally-mediated expression of a $GABA_B$ receptor subunit in gerbil auditory cortex was able to restore two auditory perceptual skills in juvenile animals reared with hearing loss, suggesting that cortical synaptic inhibition is a plausible therapeutic target for sensory processing disorders.

Introduction

Reduced cortical inhibition has been implicated in a broad range of developmental disorders including autism, schizophrenia, fragile x syndrome, and impaired sensory processing (Chao et al. 2010; Sanes & Kotak, 2011; Braat & Kooy, 2015; Gainey & Feldman, 2017). For example, visual or auditory deprivation that occurs during developmental sensitive periods leads to weaker inhibitory synapses between GABAergic interneurons and pyramidal cells in primary sensory cortices (Morales et al., 2022; Maffei et al. 2004; Takesian et al. 2012; Mowery et al., 2015). In some cases, these functional effects are correlated with a down-regulation of GABA receptors or loss of GABAergic terminals (Fuchs & Salazar, 1998; Kilman et al. 2002; Jiao et al. 2006; Sarro et al. 2008; Braat et al. 2015). Furthermore, when induced by hearing loss (HL), this reduction of inhibition has been linked to a broad range of perceptual and central processing deficits (Aizawa and Eggermont, 2007, Rosen et al., 2012; Yao and Sanes, 2018; Gay et al., 2014; Polley et al., 2013; Han et al., 2007; Kim and Bao, 2009; Zhang et al., 2001; Mowery et al., 2019). Taken together, these observations lead to the hypothesis that developmental HL induces a reduction of postsynaptic GABA receptor-mediated inhibition in auditory cortex (AC), thereby causing perceptual deficits. Here, we address a prediction that emerges from this hypothesis: increasing $GABA_A$ or $GABA_B$ receptor-dependent inhibition selectively within AC pyramidal neurons after developmental HL should restore performance on auditory perceptual tasks.

There is indirect support for the premise that normal perceptual performance is associated with appropriate levels of cortical inhibition in adults. For example, magnetic resonance spectroscopy measurements in humans demonstrate that performance on visual or auditory perceptual tasks are correlated with a higher GABA concentration (Edden et al., 2009; Dobri and Ross, 2021; Ip et al., 2021). Furthermore, a pharmacological manipulation that enhances GABAergic inhibition during behavioral testing leads to improved performance on an auditory temporal perception task in senescent gerbils and improved visual coding in senescent monkeys (Gleich et al., 2003; Leventhal et al. 2003). Consistent with this idea, systemic treatment with a GABA reuptake inhibitor can both restore the strength of inhibitory synapses following developmental HL and rescue an auditory perceptual skill (Kotak et al., 2013; Mowery et al., 2019). Although the relationship between inhibition and mature sensory processing is well established, the relative contribution of ionotropic $GABA_A$ and metabotropic $GABA_B$ postsynaptic receptors is uncertain. Depending on the outcome measure, pharmacological experiments suggest that both types of receptors can be an effective target for restoring normal function or plasticity (Iwai et al. 2003, Möhler et al., 2004; Fagiolini et al., 2004; Kotak et al., 2013; Cai et al., 2017; Zheng et al., 2012). Therefore, selective gain-of-function manipulations are required to determine whether restoring

$GABA_A$ or $GABA_B$ receptor-mediated inhibition can remediate a behavioral deficit resulting from a developmental insult.

To address this problem, we developed AAV vectors to selectively increase the functional expression of either $GABA_A$ or $GABA_B$-mediated synaptic inhibition in the AC. One virus was designed to express the α1 subunit of the $GABA_A$ receptor and the second virus was designed to express the 1b subunit of the $GABA_B$ receptor, each under the CaMKII promoter (Perez-Garci et al., 2006; Vigot et al., 2006). Our approach employed a previously validated paradigm in which transient developmental hearing loss (HL) is induced during the AC critical period, causing a reduction in $GABA_A$ and $GABA_B$-mediated AC inhibition and diminished performance on an amplitude modulation (AM) detection task (Mowery et al., 2015; Caras and Sanes, 2015; Mowery et al., 2016; Mowery et al., 2019). We also introduce a second perceptual task, spectral modulation (SM) detection, with which to assess the effect of HL and the effect of restoring inhibition. The ability to perceive spectral modulation of sound is especially important for speech and speech-in-noise comprehension (Drullman, 1995; Zeng et al. 2005). Furthermore, humans with hearing loss or cochlear implants are impaired in spectral modulation detection, and this is correlated with speech perception (Horn et al. 2017; Ozmeral et al., 2018; Nittrouer et al., 2021). Together, AM and SM cues compose two of the fundamental building blocks of natural sounds (Singh and Theunessin, 2003), and HL-induced deficits have been linked to childhood speech and language acquisition (refs). Our findings suggest that viral expression of a $GABA_B$ receptor subunit, but not a $GABA_A$ receptor subunit, in the AC can remediate the deleterious effects of developmental HL on auditory perception.

Experimental Procedures

Experimental animals: We performed behavioral experiments on 52 normal hearing and 47 transient HL gerbils (*Meriones unguiculatus*) in the age range of postnatal days (P) 10-48. For brain slice experiments, we recorded from 34 AC pyramidal neurons, obtained from a total of 8 male and female gerbils in the age range P103-169. All animals were born from breeding pairs (Charles River Laboratories) in our colony. All procedures were approved by the Institutional Animal Care and Use Committee at New York University.

Induction of transient hearing loss: Reversible HL was induced using earplugs made of molding clay inserted in both ears after ear canal opening, at P10, and sealed with super glue (Mowery et al., 2015; Mowery et al., 2016). Earplugs were checked daily, replaced if needed, and removed at P23. This manipulation produces a threshold shift of 15-50 dB, depending on frequency, as measured with auditory brainstem responses (Caras and Sanes, 2015), and ~25 dB at 4 kHz as measured behaviorally (Mowery et al., 2015).

Auditory cortex brain slice recordings: Thalamocortical brain slices were generated as described previously (Kotak et al., 2005; Mowery et al., 2015, 2019). Animals were deeply anesthetized (chloral hydrate, 400 mg/kg, IP) and brains dissected into 4ºC oxygenated artificial cerebrospinal fluid (ACSF, in mM: 125 NaCl, 4 KCl, 1.2 KH2PO4, 1.3 MgSO4, 24 NaHCO3, 15 glucose, 2.4 CaCl2, and 0.4 L-ascorbic acid; and bubbled with 95%O2-5%CO2 to a pH=7.4). Brains were vibratome-sectioned to obtain 300-400 µm perihorizontal auditory thalamocortical slices. The AC was identified by extracellular field responses to medial geniculate stimulation.

Whole-cell current clamp recordings were obtained (Warner PC-501A) from AC layer 2/3 pyramidal neurons at 32°C in oxygenated ACSF. Recording electrodes were fabricated from borosilicate glass (1.5 mm OD; Sutter P-97). The internal recording solution contained (in mM): 5 KCl, 127.5 K-gluconate, 10 HEPES, 2 MgCl2, 0.6 EGTA, 2 ATP, 0.3 GTP, and 5 phosphocreatine (pH 7.2 with KOH). The resistance of patch electrodes filled with internal solution was between 5-10 MΩ. Access resistance was 15-30 MΩ, and was compensated by about 70%. Recordings were digitized at 10 kHz and analyzed offline using custom Igor-based macros (IGOR, WaveMetrics, Lake Oswego, OR). All recorded neurons had a resting potential ≤-50 mV and overshooting action potentials.

Inhibitory postsynaptic potentials (IPSPs) were evoked via biphasic stimulation of layer 4 (1-10 mV, 10 s interstimulus interval) in the presence of ionotropic glutamate receptor antagonists (6,7-Dinitroquinoxaline-2,3-dione, DNQX, 20 µM; 2-amino-5-phosphonopentanoate, AP-5, 50 µM). The drugs were applied for a minimum of 8 min before recording IPSPs. Peak amplitudes of the short latency hyperpolarization (putative $GABA_A$ component) and long latency hyperpolarization (putative GABAB component) were measured from each response at a holding potential (Vhold)

of -50 mV. To assess $GABA_B$ receptor mediated IPSPs, the $GABA_A$ receptor antagonist bicuculline (10 μM) was also added to the bath. We previously verified that short- and long-latency IPSP components represented $GABA_A$ and $GABA_B$ receptor-dependent responses, respectively (see Fig 3D in Mowery et al., 2019).

Behavioral training and testing: Amplitude modulation (AM) and spectral modulation (SM) depth detection thresholds were assessed with an aversive conditioning procedure (Heffner & Heffner, 1995; Kelly et al., 2006) used previously in our lab (Sarro & Sanes, 2011; Rosen et al., 2012; Buran et al., 2014; Caras and Sanes, 2015, 2017, 2019). The apparatus was controlled by custom Matlab scripts, interfaced with a digital signal processor (TDT). Stimuli were delivered via a calibrated tweeter (KEF electronics) positioned above a test cage which contains a metal water spout and floor plate. Water delivery was initiated by a syringe pump (Yale Apparatus) triggered by infrared detection of spout contact. The speaker and cage were located in a sound attenuation chamber and observed via video monitor. After placement on controlled water access, gerbils learned to drink steadily from the lick spout while in the presence of continuous, unmodulated, band-limited noise (0.1-20 kHz). Separate groups of animals were trained to withdraw from the spout when the sound changed from unmodulated noise (the “safe” cue) to either AM or SM noise (the “warn” cue) by pairing the modulation with a mild shock (0.5-1.0 mA, 300 ms; Lafayette Instruments) delivered through the spout. For the AM task, procedural training was conducted with a warn cue of 0 dB re: 100% modulation depth. For the SM task, procedural training was conducted with a warn cue of 40 dB modulation depth. Repeated pairings of the shock and the warn cue resulted in a rapidly learned association and reliable spout withdrawal, which was used as a behavioral measure of modulation detection. Warn trials were interspersed with 2-6 safe trials (2-6 seconds), during which the unmodulated sound continued unchanged; the unpredictable nature of the warn presentation prevented temporal conditioning.

After the initial associative learning, five AM or SM depths, bracketing the threshold (AM task: -3 to -27 dB re: 100% depth in 3 dB steps; SM task: +3 to 27 dB), were presented in descending order. Note that AM depth was calculated relative to a completely modulated sinusoidal waveform (dB re: 100% depth), such that larger negative values represent depths that are more difficult to detect. SM depth was calculated relative to unmodulated noise, such that smaller positive values represent depths that are more difficult to detect (dB re: 0% depth). Average stimulus level was held constant at 45 dB SPL to ensure that detection was based on the modulation cue. SM stimuli were generated using 3200 random-phase sinusoidal components spaced between 0.1 and 20kHz at a sampling rate of 44.8Khz (code courtesy of Dr. Donal Sinex). Stimuli were 1 second long with a 20 ms on and off ramps. Stimuli were generated at 2 or 10 cycles/octave. For experiments testing the effects of HL and viral vectors, SM density (2 cycles/octave) and AM rate

(5 Hz) remained constant. Psychometric testing spanned 7 or 10 consecutive days. On warn trials, the response was scored as a hit when animals withdrew from the spout. On safe trials, the response was scored as a false alarm when animals incorrectly withdrew from the spout. These responses were used to calculate d' as z(hits)-z(false alarms), a signal detection metric that accounts for individual guessing rates (Green, 1966). Values were fit with psychometric functions and used to calculate thresholds (Wichmann & Hill, 2001a, 2001b). Threshold was defined as the smallest stimulus depth at which d' = 1.

Development of viral vectors: Two viral vectors were developed to express either the postsynaptic $GABA_B$ 1b subunit (Billinton et al., 1999), or the $GABA_A$ α1 subunit under the CaMKII promoter. The gene sequences for each (*Gabbr1b* and *Gabra1*) were extracted from the gerbil genome using BLAST (Zorio et al., 2019). For the *Gabbr1b* sequence, results were missing the first 141 bp of the full gene sequence, which were replaced with a sequence from the mouse to generate a complete gene sequence. These genes were inserted into viral cassettes with fluorescent reporters. At 2532 base pairs, the *Gabbr1b* sequence was too long to be used in the same cassette used for the $GABA_A$ subunit while maintaining high expression levels in an AAV1 serotype. We therefore minimized cassette length by using TurboRFP as the fluorescent reporter, WPRE3 as a posttranscriptional regulatory element, and P2A to cleave the fluorescent reporter (Merzlyak et al., 2007; Choi et al., 2014, Zufferey et al., 1999; Szymczak et al., 2005). Genes were synthesized (*Gabra1*: ThermoFisher; *Gabbr1b*: Genewiz), and the full plasmids were generated, cloned, and packaged (Penn Vector Core): AAV1.CaMKII0.4.Gabbr1b.P2A.TurboRFP.WPRE3.rBG ($4x10^{12}$ viral particles/mL), and AAV1.CaMKII0.4.Gabra1.IRES.mCherrry.WPRE.rBG ($7x10^{12}$ viral particles/mL).

Virus injections: For all animals, bilateral surgical virus injections into the AC were performed on P23 or P24, after earplug removal. AAV1.hSyn.eGFP.WPRE.bG ($5×10^{12}$ vg/mL) was used as a control. Animals were anesthetized with isoflurane, and incisions made just ventral to the temporal ridge. A small burr hole (0.7 mm diameter) was drilled in the skull ~1.4 mm below the temporal ridge, just over the AC (Radtke-Schuller et al., 2016). Virus was loaded into a glass pipette backfilled with mineral oil. The glass pipettes were made sharp enough to penetrate dura without causing damage and were inserted to a depth of 400 µm. Virus was injected at a rate of 2 nl/s with a Nanoject III (Drummond), followed by a 5 min period to permit diffusion. For the two custom viruses, a volume of 600 µl was injected, whereas for the control *GFP* virus, a volume of 250 µl was injected. Incisions were closed with surgical adhesive and the animal permitted to recover for 7 days.

Histology: At the end of each experiment, animals were deeply anesthetized with Euthasol and perfused transcardially with ice-cold PBS followed by 4% paraformaldehyde. Brains were

186 removed and fixed in the same fixative overnight at 4°C. Brains were cryoprotected and sectioned
187 (70 µm) on a vibratome and processed for fluorescence imaging. Only animals exhibiting
188 TurboRFP, mCherry or GFP properly targeted to AC were included in the behavioral data.

189 Statistical analysis. When data were normally distributed (as assessed by the Shapiro-Wilk W
190 Test), values were given as mean ± SEM. Statistical analyses were conducted using MatLab. To
191 compare multiple measures obtained from the same animal, a linear mixed effects model,
192 correcting for subject identity (formula: threshold ~ 1 + group * training day + (1 | subject)) was
193 used to verify a main effect of treatment group or the interaction between training day and
194 treatment group. For individual training days, group comparisons of variables were made using a
195 one-way analysis of variance (ANOVA) followed by least significant differences post-hoc. The HL
196 + GFP group was specified as the control group for all post hoc tests. The best threshold achieved
197 by each animal during 7 or 10 days of psychometric testing (depending on the experiment) was
198 used to determine perceptual thresholds. The significance level was set at $\alpha = 5\%$. All data are
199 expressed as mean ± SEM unless otherwise stated.

Results

To investigate the causal relationship between AC synaptic inhibition and HL-induced perceptual deficits, we developed viral vectors to express the gerbil gene sequences for subunit α1 of the $GABA_A$ receptor (*Gabra1*) or subunit 1b of the $GABA_B$ receptor (*Gabbr1b*), each under a CAMKII promoter (see Methods). Our reasoning was that overexpression of a single subunit of either receptor would remove a rate limiting step in the surface expression of the functional multimeric receptor, thereby increasing IPSP amplitude.

Functional assessment of virally expressed $GABA_A$ and $GABA_B$ receptor subunits

To determine whether each viral vector led to functional upregulation of cortical inhibitory postsynaptic potentials (IPSPs), we performed whole cell current clamp recordings from pyramidal neurons in auditory cortex brain slices 21-27 days after virus injection into AC (Figure 1A; see Methods). IPSPs were elicited in response to local electrical stimulation, as described previously (Mowery et al., 2016; Mowery et al., 2019). Figure 1B shows the vector used to express the *Gabra1* subunit under a CaMKII promoter, and a fluorescence image of the reporter molecule, mCherry, as observed during whole cell recordings. Figure 1C shows representative IPSPs recorded from a *Gabra1*-infected (orange trace; yellow pipet in panel B) and an uninfected AC neuron (gray trace) at a holding potential (V_{hold}) of -50 mV in the presence of glutamate receptor blockers (20 μM DNQX; 50 μM AP-5). Figure 1D shows that the peak amplitudes of the short latency IPSP hyperpolarization (putative $GABA_A$ component, labeled "A") was significantly greater for infected neurons (Mean ± SEM; infected: 12.8 ± 0.6 mV; uninfected: 6.8 ± 0.6 mV; $q=2.05$, $df=26$, $p<0.0001$). Therefore, the *Gabra1* vector increased $GABA_A$ receptor-mediated IPSP amplitude in AC pyramidal neurons.

Figure 1E shows the vector used to express the postsynaptic *Gabbr1b* subunit (Billinton et al., 1999) under a CamKII promoter, and a fluorescence image of the reporter molecule, turboRFP, as observed during whole cell recordings. Figure 1F shows representative IPSPs recorded from a *Gabbr1b*-infected (blue trace; yellow pipet in panel E) and an uninfected AC neuron (gray trace) at a holding potential (V_{hold}) of -50 mV in the presence of glutamate receptor antagonists (20 μM DNQX; 50 μM AP-5) and a $GABA_A$ receptor antagonist (10 μM bicuculline). Figure 1G shows that the peak amplitudes of the long latency IPSP hyperpolarization (putative $GABA_B$ component, labeled "B") was significantly greater for infected neurons (Mean ± SEM; infected: 8.7 ± 0.6 mV; uninfected: 5.8 ± 0.4 mV; $q=2.03$, $df=32$, $p=0.0002$). Therefore, the Gabbr1b vector increased $GABA_B$ receptor-mediated IPSP amplitude in AC pyramidal neurons.

Assessing perceptual performance on AM and SM tasks

Figure 2 outlines the full experimental protocol**.** We induced reversible developmental hearing loss, beginning at ear canal opening (P10) and ending after the auditory critical period (P23) by

inserting earplugs (Figure 2A, orange shading), as described previously (Caras and Sanes, 2015). We injected separate groups of HL-reared animals with the *Gabra1* (n = 8) or *Gabbr1b*-expressing vector (n = 9), or a GFP control virus (n = 9), bilaterally in AC between P23 and P25, after earplug removal. We also included a normal hearing group (n = 15; Figure 2A, gray shading). Following a 7 day recovery period, animals were water restricted and began behavioral training on P30.

Separate groups of animals were tested on AM depth detection (Sarro and Sanes, 2011; Rosen et al., 2012; Caras & Sanes, 2015) or SM depth detection. As described in Methods, control and HL-reared animals were trained to drink from a lick spout during continuous noise (0.1-20 kHz, 45 dB SPL). For the AM detection task, animals were initially trained to withdraw from the spout when 5 Hz amplitude modulation at 0 dB re: 100% occurred (Figure 2B, top). For the SM detection task, animals were initially trained to withdraw from the spout when 2 cycles/octave density spectral modulation at 40 dB depth occurred (Figure 2B, bottom). Procedural learning continued until animals achieved a d' $\gtrsim$ 1.3 with a 0 dB re: 100% depth AM stimuli or 40 dB depth SM stimuli (4-8 days). We then conducted 7 days of psychometric testing as animals' performance gradually improved on the AM or SM task (Figure 2C). Perceptual thresholds improved as gerbils responded to smaller modulation depths due to perceptual learning (Caras & Sanes, 2017).

We first tested the effect of HL and GABA receptor subunit expression on AM depth detection. Figure 3A presents representative psychometric functions for two individual animals and shows that AM detection was superior for the HL-reared gerbil that received bilateral AC injections of a *Gabbr1b*-expressing vector (HL+*Gabbr1b*; blue line) as compared to the HL-reared gerbil that received AC bilateral injections of a *GFP*-expressing vector (HL+*GFP*; green line). As schematized in Figure 2A, top, we obtained thresholds for animals in these two groups, as well as HL-reared animals that received a *Gabra1*-expressing vector (HL+*Gabra1*), and normal hearing (NH) animals.

Figure 3B shows thresholds by group over 7 days of psychometric testing. A linear mixed-effects model comparing the effects of training day and virus condition on thresholds, and taking into account individual subject behavior, indicates that viral treatment was a significant factor ($F = 10.83$, $p = 9.83 \times 10^{-7}$). Therefore, expression of the *Gabbr1b* subunit restored normal behavioral performance on the AM detection task in HL-reared animals in a manner that was independent of training day.

There was a significant effect of treatment group on day 1 of perceptual testing (one-way ANOVA, $p = 4.02 \times 10^{-5}$, $F = 10.46$, $df = 40$, Figure 3C) and day 7 of perceptual testing (one-way ANOVA, $p = 6.85 \times 10^{-8}$, $F = 20.07$, $df = 40$, Figure 3D). A post hoc comparison revealed that AM detection thresholds were significantly poorer for transient HL-reared animals that received a control virus (HL+*GFP*) as compared to normal hearing animals (NH). This was the case both for day 1

(HL+*GFP* = -5.61 ± 0.99 dB, NH = -10.94 ± 0.77 dB, p = 8.35 x 10^{-4}) and day 7 of testing (HL+*GFP* = -8.90 ± 0.91 dB, NH = -14.56 ± 0.70 dB, p = 1.00 x 10^{-4}). This finding confirms the effect of HL reported previously (Caras and Sanes, 2015; Mowery et al., 2019).

Post hoc comparisons also revealed that $GABA_B$ subunit expression, but not $GABA_A$ receptor expression could partially restore AM detection thresholds in HL-reared animals. Animals in the HL+*Gabbr1b* group displayed significantly lower AM detection thresholds than the HL+*GFP* group, both at day 1 (HL+*Gabbr1b* = -10.37 ± 0.99 dB, p = 0.009, NH = -10.94 ± 0.77 dB, p = 8.35 x 10^{-4}) and day 7 of perceptual testing (HL+*Gabbr1b* = -12.47 ± 0.91 dB, p = 0.04). In contrast, the HL+*Gabra1* group did not different significantly from the HL+*GFP* group, either at day 1 (HL+*GFP* = -5.61 ± 0.99 dB, HL+*Gabra1* = -5.24 ± 1.06 dB, p = .99), or day 7 of perceptual testing (HL+*GFP* = -8.90 ± 0.91 dB, HL+*Gabra1* = -6.01 ± 0.96 dB, p = .15).

SM detection performance in normal hearing gerbils

To develop a behavioral test of perception of spectral modulation (SM), we modified the aversive conditioning paradigm such that unmodulated white noise transitioned to spectrally modulated noise on “warn” trials. Similar to the AM detection task, SM stimuli were presented at multiple depths in 3 dB increments to determine each animal’s perceptual threshold. Since SM detection has not been assessed previously in gerbils, we first sought to validate two features of this psychometric task. SM is described by a density (cycles/octave) which specifies the peak-to-trough distance of the logarithmic sinusoidal frequency filter used. Humans achieve their best thresholds in the range of 2-4 cycles/octave and thresholds increase at 10 cycles/octave (Eddins and Bero, 2007). We trained gerbils on the same aversive conditioning paradigm used for AM, but with the change cue being a SM stimulus at either 2 or 10 cycles/octave. We found that best thresholds achieved during 10 days of psychometric testing were significantly lower at 2 cycles/octave (5.4 ± 1.43 dB, n = 14) than 10 (8.3 ± 2.5 dB; p = 0.363, t = -2.148, df = 11, unpaired t-test, n = 8; Figure S1). Therefore, all subsequent SM detection psychometric tests used 2 cycles/octave. To confirm that gerbil SM detection is robust to changes in level, as reported fo humans (Eddins and Bero, 2007), we alternated between 45 dB SPL and 36 dB SPL during 4 additional days of testing with 2 cycles/octave stimuli (n = 8). There was no significant difference in thresholds over each pair of testing days (45 dB days: 9.2 ± 4.0 dB, 36 dB days: 10.66 ± 5.03 dB, p = 0.562, t = 0.593, df = 14, paired t-test). This indicates that gerbil perception of SM stimuli is similar to that displayed by humans.

***Gabbr1b* expression restores SM detection following developmental hearing loss**

We next tested the effect of HL on SM depth detection, and the ability of GABA receptor expression to rescue a HL-induced perceptual deficit. Figure 4A presents representative psychometric functions for two individual animals and shows that SM detection was superior for

the HL-reared gerbil that received bilateral AC injections of a *Gabbr1b*-expressing vector (HL+*Gabbr1b*; blue line) as compared to the HL-reared gerbil that received AC bilateral injections of a *GFP*-expressing vector (HL+*GFP*; green line). As schematized in Figure 2A, bottom, we obtained thresholds for animals in these two groups, as well as HL-reared animals that received a *Gabra1*-expressing vector (HL+*Gabra1*), and normal hearing (NH) animals (HL+*GFP*, n = 8; HL+*Gabra1*, n = 7; HL+*Gabbr1b*, n = 6; NH+*GFP*, n = 7). As observed previously with procedural training on the AM detection task, all 4 groups reached criterion in a similar number of trials and reached similar maximum d' on the SM detection task (Figure S2).

Figure 4B shows group thresholds over all 7 days of training. A linear mixed effects model shows that viral treatment alone is not a significant factor ($F = 0.634$, $p = 0.594$) but the interaction between group and training day was ($F = 13.257$, $p = 7.64 \times 10^{-8}$). Therefore, expression of the *Gabbr1b* subunit restores normal threshold improvement trends on the SM detection task in HL-reared animals.

The SM detection thresholds of all four groups did not differ significantly from one another on day 1 of psychometric testing (HL+*GFP*: dB = 20.66 ± 2.11; HL+*Gabra1*: dB = 21.38 ± 2.11; HL+*Gabbr1b*: dB = 20.83 ± 2.31; NH+GFP: dB = 20.77 ± 1.96; ANOVA, $p = .9951$, $F = 0.02$, $df = 23$, Figure 4C). However, as shown in Figure 4D, a significant effect of treatment group emerged by day 7 of testing (one-way ANOVA, $p = 1.34 \times 10^{-5}$, $F = 14.5$, $df = 27$). NH+*GFP* and HL+*Gabbr1b* animals both reached low thresholds of 7.8 ± 1.6 dB and 8.0 ± 1.8 dB, respectively. In contrast, thresholds for HL+*GFP* (17.5 ± 1.5 dB) and HL+*Gabra1* (19.6 ± 1.6 dB) animals improved very little over 7 days of testing. There was no significant difference between day 7 thresholds for HL+*Gabbr1b* and NH+*GFP* animals and both were significantly better than HL+*GFP* ($p = 0.002$, $p = 0.0011$, respectively).

Discussion

Proper regulation of synaptic inhibition is integral to the development and maintenance of sensory processing. Transient or permanent developmental HL that begins during an AC critical period causes a long-lasting reduction of cortical synaptic inhibition that is attributable to the functional loss of both ionotropic $GABA_A$ and metabotropic $GABA_B$ receptors (Kotak et al., 2005; Takesian et al., 2012; Mowery et al., 2019). This reduction of AC inhibition correlates with impairments in psychometric performance on a range of auditory tasks as well as degraded AC neuron stimulus processing (Rosen et al., 2012; Buran et al., 2014; Caras and Sanes, 2015; Ihlefeld et al., 2016; von Trapp et al., 2017; Yao & Sanes, 2018). To test whether there is a causal relationship between AC inhibition and perceptual skills, we upregulated GABA receptor-mediated inhibition in AC pyramidal neurons through viral expression of the *Gabra1* or *Gabbr1b* subunit genes in animals reared with HL. Our results show that upregulating $GABA_B$ receptor-dependent inhibition through expression of the gerbil *Gabbr1b* subunit gene can rescue two different perceptual deficits, AM and SM detection. In contrast, upregulating $GABA_A$ receptor-mediated inhibition through expression of the gerbil *Gabra1* subunit gene had no effect on perceptual performance. Therefore, our results suggest that the magnitude of AC inhibition is positively correlated with perceptual performance, with postsynaptic $GABA_B$ receptors playing a pivotal role.

Amplitude and spectral modulation are discrete features of natural sounds, including speech, and sensitivity to these cues is correlated with speech comprehension (Cazals et al., 1994; Shannon et al., 1995; Singh and Theunissen, 2003; Elliott 2009; Nittrouer et al., 2021). Here we developed a behavioral paradigm to assess SM detection in gerbils, such that the effects of HL could be compared with a previously characterized percept, AM detection (Rosen et al., 2012; Caras & Sanes, 2015). We found that rearing conditions and viral treatment had no effect on procedural training times, in agreement with past results with our AM paradigm, although training times were comparatively longer (Figure 2S). Adult humans display depth detection thresholds of ~2 dB at 2 cycles/octave, with poorer performance at higher spectral densities (Eddins and Bero, 2007). In agreement, we found that gerbils have better thresholds at 2 cycles/octave than 10 cycles/octave and that best thresholds are within 3 dB of human performance at 2 cycles/octave (Figure 1S). We also analyzed a concatenated series of hundreds of gerbil vocalizations and found that spectral modulation drops off significantly above 2 cycles/octave (not shown). This validates our use of a new perceptual test with which to assess the impact of hearing loss and the capacity of treatments to restore perception.

Interpreting the pattern of restored AM and SM detection following *Gabbr1b* expression

Gabbr1b expression rescued AM and SM detection in HL-reared animals, but with different magnitudes and time courses. For the AM detection task *Gabbr1b*-treatment improved perceptual

363 performance in HL-reared animals from the first day of testing as compared to GFP-treated
364 controls (Figure 3). This improved performance was maintained during the 7 days of testing. This
365 outcome is consistent with a rapid improvement in AM stimulus encoding following *Gabbr1b*
366 expression, but no effect on perceptual learning (i.e., an improvement in detection threshold as a
367 result of practice). In contrast, *Gabbr1b* expression led to a gradual improvement of SM thresholds
368 during the 7 days of testing, identical to NH animals with GFP expression (Figure 4). In principle,
369 these differences in the effect of restoring inhibition could relate to differences in the way that AM
370 and SM stimuli are represented in the AC.
371 Amplitude and spectrally modulated noise are expected to differ in terms of the evoked discharge
372 pattern of AC neurons. AM stimuli are known to produce a strong temporal response that
373 correlates with the AM rate. In contrast, SM stimuli produce a response that is dependent on
374 frequency tuning (e.g., inhibitory sidebands) (Calhoun & Schreiner, 1994, 1998; Atencio &
375 Schreiner, 2010). At the cellular level, one possibility is that feedforward inhibition mediated by
376 Parvalbumin-expressing interneurons tightens the timing of the auditory evoked response in the
377 input Layer 4/5 (Wehr and Zador, 2003; Nocon et al., 2022), which may contribute to perception
378 of amplitude modulation. In contrast, SM stimuli are stationary. Here, intracortical pathways may
379 recruit local interneurons that mediate lateral inhibition, increasing gain in Layer 2/3, thereby
380 improving the detection of energy differences across spectral bands (Kaur et al., 2004; Kaur et
381 al., 2005; Li et. al. 2014).

382 **Relationship of GABA receptor manipulation to the AC critical period**
383 In the current experiments, the manipulations and behavioral assays all occur prior to sexual
384 maturation, a time during which inhibitory functional properties continue to mature (Pinto et al.,
385 2010; Takesian et al., 2012). A large body of research from the developing visual pathway shows
386 that inhibitory synapse development regulates cortical plasticity. Monocular deprivation (MD)
387 leads to reduced cortical activation by the deprived eye during a developmental CP, and
388 experimentally increasing GABAergic transmission can close the critical period prematurely
389 (reviews: Hensch, 2004; Hensch, 2005; Hooks and Chen, 2007). One implication of these
390 observations is that inhibition in adult animals is too strong to permit plasticity. In fact,
391 manipulations that reduce cortical inhibition in adults can induce excitatory synaptic plasticity (He
392 et al., 2006; Sale et al., 2007; Fernandez et al., 2007; Harauzov et al., 2010). Therefore, when
393 inhibitory strength is high, behavioral deficits can be ameliorated by temporarily lowering it. In
394 contrast, our results suggest that when inhibitory strength is low, as occurs after developmental
395 HL, behavioral deficits can be ameliorated by permanently raising it.
396 The gerbil AC displays a well characterized critical period (CP) for the effect of HL that closes at
397 P18 (Mowery et al., 2015). When HL is initiated after P18, there is no reduction to AC inhibitory

synapse strength (Mowery et al., 2016). In contrast, when HL is initiated before P18, the reduction of AC inhibitory synapse strength persists to adulthood and can be attributed to the functional loss of both $GABA_A$ and $GABA_B$ receptor-mediated IPSPs (Mowery et al., 2019). Therefore, a core premise of this study is that the loss of one or both forms of postsynaptic inhibition is causally related to perceptual deficits that attend developmental HL. Since the virus was injected into AC on P23, our results suggest that the manipulation need not occur during the cortical CP in order to restore normal neural and behavioral function. This is consistent with our finding that systemic treatment with a GABA reuptake inhibitor (SGRI) from P23-35 also rescues AC inhibition and AM detection thresholds (see Fig 2e in Mowery et al., 2019).

Since a reduction of $GABA_A$ receptor mediated inhibition has been implicated in many developmental disorders, it was reasonable to predict that upregulating inhibitory strength through *Gabra1* expression (Figure 1D) would rescue HL-induced deficits on auditory tasks. However, we previously reported that systemic treatment with a $GABA_A$ α1 receptor agonist, zolpidem, does not restore AM detection thresholds following development HL (see Fig 2f in Mowery et al., 2019). Two lines of evidence may explain why perceptual performance was rescued only by upregulating $GABA_B$ receptor-mediated inhibition. First, $GABA_B$ receptor function may have a direct impact on synaptic plasticity, particularly during development. Postsynaptic $GABA_B$ receptors can induce inhibitory long-term depression (iLTD) at feedforward inhibitory synapses between Parvalbumin-expressing interneurons and Pyramidal neurons in input layers of visual cortex during a developmental CP (Wang and Maffei, 2014). This mechanism has been implicated in auditory map remodeling (Vickers et al., 2018), and $GABA_B$ receptor agonists enhance ocular dominance plasticity (Cai et al., 2017). Second, postsynaptic $GABA_B$ receptors are located extrasynaptically and modulate both the activity of postsynaptic $GABA_A$ receptors and NMDA receptor-driven LTP (Komatsu, 1996; Fritschy et al., 1999; Charara et al., 2005; Booker et al., 2013; Tao et al., 2013, Connelly et al. 2013). $GABA_B$ receptor activation may also induce BDNF release, thereby inducing the addition of perisomatic GABAergic synapses (Fiorentino et al., 2009). Therefore, although both forms of GABAergic inhibition are reduced by HL, dysregulation of $GABA_B$ receptor's modulatory role may have a substantial impact on the acquisition of perceptual skills during development.

Limitations to data interpretations

Expression of AAV vectors begins within one week of infusion, and typically ramps up to a plateau at 2-3 weeks (Reimsnider et al. 2007; Kaplitt et al. 1994; Chamberlin et al. 1998). Therefore, we timed our experiment such that psychometric testing fell within a 2-3 week post-injection window during which time expression should have been maximal. However, it is possible that a continued increase of expression during training was associated with a greater influence on behavioral

performance at later testing days. A second consideration is that this study used two specific inhibitory receptors, but the approach did not restrict expression to synapses from any particular type of inhibitory interneuron. Parvalbumin or Somatostatin-expressing interneurons at the thalamorecipient layer or in L2/3, which naturally target $GABA_B$ receptors each synapse onto pyramidal neurons that expressed GABBR1B protein following viral infection (Manz et al. 2019). Additionally, L2/3 Pyramidal neurons extend dendrites to L1 within which Neurogliaform interneurons form synapses that primarily evoke $GABA_B$ receptor-mediated responses and regulate plasticity (Tamás et al., 2003). Therefore, specific interneuronal connections responsible for the reported behavioral effects is unknown. Finally, it is possible that increasing inhibitory transmission could have induced homeostatic upregulation of excitation in AC and a maintenance of excitatory/inhibitory balance (Turrigiano & Nelson, 2004; Le Roux *et al.*, 2006). This potential effect could include a normalization of excitatory cellular properties and may have contributed to the behavioral benefits of our manipulation. In fact, $GABA_A$ receptors have been shown to regulate homeostatic plasticity and this may explain why expressing GABRA1 did not improve performance (Wen et al. 2022; Le Roux et al. 2008; Rannals & Kapur, 2011).

Conclusion

Here we have shown that restoring inhibition in AC alone was sufficient to restore auditory perception after a developmental insult. Restoring cortical synaptic inhibition may be relevant to a range of developmental disorders. For example, GABA levels in visual cortex are reduced in amblyopia and this is correlated with weaker perceptual suppression by the amblyopic eye (Mukerji et al., 2022). By directly comparing the impact of restoring *Gabra1* and *Gabbr1b* protein expression we have shown that this effect was only achieved by upregulating $GABA_B$ receptor-mediated inhibition. This result is surprising given a long focus on $GABA_A$ receptor-mediated inhibition in the field of developmental sensory processing (Fagiolini et al. 2004; Chang et al., 2005). Our findings suggest that regulating $GABA_B$ receptor mediated inhibition remains a plausible target for therapies that seek to prevent or reverse behavioral deficits that attend developmental disorders.

References

Aizawa, N., & Eggermont, J. J. (2007). Mild noise-induced hearing loss at young age affects temporal modulation transfer functions in adult cat primary auditory cortex. *Hearing research*, *223*(1-2), 71-82.

Anbuhl, K. L., Yao, J. D., Hotz, R. A., Mowery, T. M., & Sanes, D. H. (2022). Auditory processing remains sensitive to environmental experience during adolescence in a rodent model. *Nature communications*, *13*(1), 1-17.

Atencio, C. A., & Schreiner, C. E. (2010). Laminar diversity of dynamic sound processing in cat primary auditory cortex. Journal of neurophysiology, 103(1), 192-205.

Billinton, A., Upton, N., & Bowery, N. G. (1999). GABAB receptor isoforms GBR1a and GBR1b, appear to be associated with pre-and post-synaptic elements respectively in rat and human cerebellum. *British journal of pharmacology*, *126*(6), 1387-1392.

Booker, S. A., Gross, A., Althof, D., Shigemoto, R., Bettler, B., Frotscher, M., ... & Vida, I. (2013). Differential GABAB-receptor-mediated effects in perisomatic-and dendrite-targeting parvalbumin interneurons. *Journal of Neuroscience*, *33*(18), 7961-7974.

Braat, S., & Kooy, R. F. (2015). The GABAA receptor as a therapeutic target for neurodevelopmental disorders. *Neuron*, *86*(5), 1119-1130.

Buran, B. N., Sarro, E. C., Manno, F. A., Kang, R., Caras, M. L., & Sanes, D. H. (2014). A sensitive period for the impact of hearing loss on auditory perception. *Journal of Neuroscience*, *34*(6), 2276-2284.

Cai, S., Fischer, Q. S., He, Y., Zhang, L., Liu, H., Daw, N. W., & Yang, Y. (2017). GABAB receptor-dependent bidirectional regulation of critical period ocular dominance plasticity in cats. *PLoS One*, *12*(6), e0180162.

Schreiner, C.E. & Calhoun, B.M. (1994) Spectral envelope coding in cat primary auditory cortex: Properties of ripple transfer functions. Aud.Neurosci.,1, 39–61.

Calhoun, B. M., & Schreiner, C. E. (1998). Spectral envelope coding in cat primary auditory cortex: linear and non-linear effects of stimulus characteristics. European Journal of Neuroscience, 10(3), 926-940.

Caras, M. L., & Sanes, D. H. (2015). Sustained perceptual deficits from transient sensory deprivation. *Journal of Neuroscience*, *35*(30), 10831-10842.

Caras, M. L., & Sanes, D. H. (2017). Top-down modulation of sensory cortex gates perceptual learning. Proceedings of the National Academy of Sciences, 114(37), 9972-9977.

Caras, M. L., & Sanes, D. H. (2019). Neural variability limits adolescent skill learning. Journal of Neuroscience, 39(15), 2889-2902.

Cazals, Y., Pelizzone, M., Saudan, O., & Boex, C. (1994). Low-pass filtering in amplitude modulation detection associated with vowel and consonant identification in subjects with cochlear implants. *The Journal of the Acoustical Society of America*, *96*(4), 2048-2054.

Chamberlin, N. L., Du, B., de Lacalle, S., & Saper, C. B. (1998). Recombinant adeno-associated virus vector: use for transgene expression and anterograde tract tracing in the CNS. Brain research, 793(1-2), 169-175.

Chang, E. F., Bao, S., Imaizumi, K., Schreiner, C. E., & Merzenich, M. M. (2005). Development of spectral and temporal response selectivity in the auditory cortex. Proceedings of the National Academy of Sciences, 102(45), 16460-16465.

Charara, A., Pare, J. F., Levey, A. I., & Smith, Y. (2005). Synaptic and extrasynaptic GABA-A and GABA-B receptors in the globus pallidus: an electron microscopic immunogold analysis in monkeys. *Neuroscience*, *131*(4), 917-933.

Choi, J.-H., Yu, N.-K., Baek, G.-C., Bakes, J., Seo, D., Nam, H. J., Baek, S. H., Lim, C.-S., Lee, Y.-S., & Kaang, B.-K. (2014). Optimization of AAV expression cassettes to improve packaging capacity and transgene expression in neurons. *Molecular brain*, *7*(1), 1-10.

Connelly, W. M., Fyson, S. J., Errington, A. C., McCafferty, C. P., Cope, D. W., Di Giovanni, G., & Crunelli, V. (2013). GABAB receptors regulate extrasynaptic GABAA receptors. *Journal of Neuroscience*, *33*(9), 3780-3785.

Dobri, S. G., & Ross, B. (2021). Total GABA level in human auditory cortex is associated with speech-in-noise understanding in older age. *Neuroimage*, *225*, 117474.

Drullman, R. (1995). Temporal envelope and fine structure cues for speech intelligibility. The Journal of the Acoustical Society of America, 97(1), 585-592.

Edden, R. A., Muthukumaraswamy, S. D., Freeman, T. C., & Singh, K. D. (2009). Orientation discrimination performance is predicted by GABA concentration and gamma oscillation frequency in human primary visual cortex. *Journal of Neuroscience*, *29*(50), 15721-15726.

Eddins, D. A., & Bero, E. M. (2007). Spectral modulation detection as a function of modulation frequency, carrier bandwidth, and carrier frequency region. *The Journal of the Acoustical Society of America*, *121*(1), 363-372.

Fagiolini, M., Fritschy, J. M., Low, K., Mohler, H., Rudolph, U., & Hensch, T. K. (2004). Specific GABAA circuits for visual cortical plasticity. *Science*, *303*(5664), 1681-1683.

Fernandez, F., Morishita, W., Zuniga, E., Nguyen, J., Blank, M., Malenka, R. C., & Garner, C. C. (2007). Pharmacotherapy for cognitive impairment in a mouse model of Down syndrome. Nature neuroscience, 10(4), 411-413.

Fiorentino H, Kuczewski N, Diabira D, Ferrand N, Pangalos MN, Porcher C, Gaiarsa JL (2009) GABA(B) receptor activation triggers BDNF release and promotes the maturation of GABAergic synapses. J Neurosci 29: 11650-11661.

Fritschy, J. M., Meskenaite, V., Weinmann, O., Honer, M., Benke, D., & Mohler, H. (1999). GABAB-receptor splice variants GB1a and GB1b in rat brain: developmental regulation, cellular distribution and extrasynaptic localization. *European Journal of Neuroscience*, *11*(3), 761-768.

Fuchs, J. L., & Salazar, E. (1998). Effects of whisker trimming on GABAA receptor binding in the barrel cortex of developing and adult rats. *Journal of Comparative Neurology*, *395*(2), 209-216.

Gainey, M. A., & Feldman, D. E. (2017). Multiple shared mechanisms for homeostatic plasticity in rodent somatosensory and visual cortex. *Philosophical Transactions of the Royal Society B: Biological Sciences*, *372*(1715), 20160157.

Gay, J. D., Voytenko, S. V., Galazyuk, A. V., & Rosen, M. J. (2014). Developmental hearing loss impairs signal detection in noise: putative central mechanisms. *Frontiers in systems neuroscience*, *8*, 162.

Gleich, O., Hamann, I., Klump, G. M., Kittel, M., & Strutz, J. (2003). Boosting GABA improves impaired auditory temporal resolution in the gerbil. *Neuroreport*, *14*(14), 1877-1880.

Han, Y. K., Köver, H., Insanally, M. N., Semerdjian, J. H., & Bao, S. (2007). Early experience impairs perceptual discrimination. *Nature neuroscience*, *10*(9), 1191-1197.

Harauzov, A., Spolidoro, M., DiCristo, G., De Pasquale, R., Cancedda, L., Pizzorusso, T., ... & Maffei, L. (2010). Reducing intracortical inhibition in the adult visual cortex promotes ocular dominance plasticity. *Journal of Neuroscience*, *30*(1), 361-371.

He, H. Y., Hodos, W., & Quinlan, E. M. (2006). Visual deprivation reactivates rapid ocular dominance plasticity in adult visual cortex. *Journal of Neuroscience*, *26*(11), 2951-2955.

Hensch, T. K. (2004). Critical period regulation. *Annu. Rev. Neurosci.*, *27*, 549-579.

Hensch, T. K. (2005). Critical period plasticity in local cortical circuits. *Nature Reviews Neuroscience*, *6*(11), 877-888.

Hooks, B. M., & Chen, C. (2007). Critical periods in the visual system: changing views for a model of experience-dependent plasticity. *Neuron*, *56*(2), 312-326.

Horn, D. L., Dudley, D. J., Dedhia, K., Nie, K., Drennan, W. R., Won, J. H., ... & Werner, L. A. (2017). Effects of age and hearing mechanism on spectral resolution in normal hearing and cochlear-implanted listeners. *The Journal of the Acoustical Society of America*, *141*(1), 613-623.

Ihlefeld, A., Chen, Y. W., & Sanes, D. H. (2016). Developmental conductive hearing loss reduces modulation masking release. *Trends in hearing*, *20*, 2331216516676255.

Ip, I. B., Emir, U. E., Lunghi, C., Parker, A. J., & Bridge, H. (2021). GABAergic inhibition in the human visual cortex relates to eye dominance. *Scientific reports*, *11*(1), 1-11.

Iwai, Y., Fagiolini, M., Obata, K., & Hensch, T. K. (2003). Rapid critical period induction by tonic inhibition in visual cortex. *Journal of Neuroscience*, *23*(17), 6695-6702.

Jiao, Y., Zhang, C., Yanagawa, Y., & Sun, Q. Q. (2006). Major effects of sensory experiences on the neocortical inhibitory circuits. *Journal of Neuroscience*, *26*(34), 8691-8701.

Kaplitt, M. G., Leone, P., Samulski, R. J., Xiao, X., Pfaff, D. W., O'Malley, K. L., & During, M. J. (1994). Long-term gene expression and phenotypic correction using adeno-associated virus vectors in the mammalian brain. Nature genetics, 8(2), 148-154.

Kaur, S., Lazar, R., & Metherate, R. (2004). Intracortical pathways determine breadth of subthreshold frequency receptive fields in primary auditory cortex. *Journal of neurophysiology*, *91*(6), 2551-2567.

Kaur, S., Rose, H. J., Lazar, R., Liang, K., & Metherate, R. (2005). Spectral integration in primary auditory cortex: laminar processing of afferent input, in vivo and in vitro. *Neuroscience*, *134*(3), 1033-1045.

Kilman, V., Van Rossum, M. C., & Turrigiano, G. G. (2002). Activity deprivation reduces miniature IPSC amplitude by decreasing the number of postsynaptic GABAA receptors clustered at neocortical synapses. *Journal of Neuroscience*, *22*(4), 1328-1337.

Kim, H., & Bao, S. (2009). Selective increase in representations of sounds repeated at an ethological rate. *Journal of Neuroscience*, *29*(16), 5163-5169.

Komatsu, Y. (1996). GABAB receptors, monoamine receptors, and postsynaptic inositol trisphosphate-induced Ca2+ release are involved in the induction of long-term potentiation at visual cortical inhibitory synapses. *Journal of Neuroscience*, *16*(20), 6342-6352.

Kotak, V. C., Fujisawa, S., Lee, F. A., Karthikeyan, O., Aoki, C., & Sanes, D. H. (2005). Hearing loss raises excitability in the auditory cortex. *Journal of Neuroscience*, *25*(15), 3908-3918.

Kotak, V. C., Takesian, A. E., MacKenzie, P. C., & Sanes, D. H. (2013). Rescue of inhibitory synapse strength following developmental hearing loss. *PLoS One*, *8*(1), e53438.

Le Roux, N., Amar, M., Moreau, A., Baux, G., & Fossier, P. (2008). Impaired GABAergic transmission disrupts normal homeostatic plasticity in rat cortical networks. European Journal of Neuroscience, 27(12), 3244-3256.

Leventhal, A. G., Wang, Y., Pu, M., Zhou, Y., & Ma, Y. (2003). GABA and its agonists improved visual cortical function in senescent monkeys. *Science*, *300*(5620), 812-815.

Li, L. Y., Ji, X. Y., Liang, F., Li, Y. T., Xiao, Z., Tao, H. W., & Zhang, L. I. (2014). A feedforward inhibitory circuit mediates lateral refinement of sensory representation in upper layer 2/3 of mouse primary auditory cortex. *Journal of Neuroscience*, *34*(41), 13670-13683.

Maffei, A., Nelson, S. B., & Turrigiano, G. G. (2004). Selective reconfiguration of layer 4 visual cortical circuitry by visual deprivation. *Nature neuroscience*, *7*(12), 1353-1359.

Manz, K. M., Baxley, A. G., Zurawski, Z., Hamm, H. E., & Grueter, B. A. (2019). Heterosynaptic GABAB receptor function within feedforward microcircuits gates glutamatergic transmission in the nucleus accumbens core. *Journal of Neuroscience*, *39*(47), 9277-9293.

Mentch, J., Spiegel, A., Ricciardi, C., & Robertson, C. E. (2019). GABAergic inhibition gates perceptual awareness during binocular rivalry. *Journal of Neuroscience*, *39*(42), 8398-8407.

Merzlyak, E. M., Goedhart, J., Shcherbo, D., Bulina, M. E., Shcheglov, A. S., Fradkov, A. F., ... & Chudakov, D. M. (2007). Bright monomeric red fluorescent protein with an extended fluorescence lifetime. *Nature methods*, *4*(7), 555-557.

Möhler, H., Fritschy, J. M., Crestani, F., Hensch, T., & Rudolph, U. (2004). Specific GABAA circuits in brain development and therapy. *Biochemical pharmacology*, *68*(8), 1685-1690.

Mowery, T. M., Caras, M. L., Hassan, S. I., Wang, D. J., Dimidschstein, J., Fishell, G., & Sanes, D. H. (2019). Preserving inhibition during developmental hearing loss rescues auditory learning and perception. *Journal of Neuroscience*, *39*(42), 8347-8361.

Mowery, T. M., Kotak, V. C., & Sanes, D. H. (2015). Transient hearing loss within a critical period causes persistent changes to cellular properties in adult auditory cortex. *Cerebral cortex*, *25*(8), 2083-2094.

Mowery, T. M., Kotak, V. C., & Sanes, D. H. (2016). The onset of visual experience gates auditory cortex critical periods. *Nature communications*, *7*(1), 1-11.

Mukerji, A., Byrne, K. N., Yang, E., Levi, D. M., & Silver, M. A. (2022). Visual cortical γ−aminobutyric acid and perceptual suppression in amblyopia. *Frontiers in Human Neuroscience*, *16*.

Nittrouer, S., Lowenstein, J. H., & Sinex, D. G. (2021). The contribution of spectral processing to the acquisition of phonological sensitivity by adolescent cochlear implant users and normal-hearing controls. *The Journal of the Acoustical Society of America*, *150*(3), 2116-2130.

Nocon, J. C., Gritton, H. J., James, N. M., Han, X., & Sen, K. (2022). Parvalbumin neurons, temporal coding, and cortical noise in complex scene analysis. bioRxiv, 2021-09.

Osanai, Y., Battulga, B., Yamazaki, R., Kouki, T., Yatabe, M., Mizukami, H., ... & Ohno, N. (2022). Dark rearing in the visual critical period causes structural changes in myelinated axons in the adult mouse visual pathway. *Neurochemical Research*, *47*(9), 2815-2825.

Ozmeral, E. J., Eddins, A. C., & Eddins, D. A. (2018). How do age and hearing loss impact spectral envelope perception? *Journal of Speech, Language, and Hearing Research*, *61*(9), 2376-2385.

Pérez-Garci, E., Gassmann, M., Bettler, B., & Larkum, M. E. (2006). The GABAB1b isoform mediates long-lasting inhibition of dendritic Ca2+ spikes in layer 5 somatosensory pyramidal neurons. *Neuron*, *50*(4), 603-616.

Pinto, J. G., Hornby, K. R., Jones, D. G., & Murphy, K. M. (2010). Developmental changes in GABAergic mechanisms in human visual cortex across the lifespan. Frontiers in cellular neuroscience, 16.

Polley, D. B., Thompson, J. H., & Guo, W. (2013). Brief hearing loss disrupts binaural integration during two early critical periods of auditory cortex development. *Nature communications*, *4*(1), 1-13.

Radtke-Schuller, S., Schuller, G., Angenstein, F., Grosser, O. S., Goldschmidt, J., & Budinger, E. (2016). Brain atlas of the Mongolian gerbil (Meriones unguiculatus) in CT/MRI-aided stereotaxic coordinates. *Brain Structure and Function*, *221*(1), 1-272.

Rannals, M. D., & Kapur, J. (2011). Homeostatic strengthening of inhibitory synapses is mediated by the accumulation of GABAA receptors. Journal of Neuroscience, 31(48), 17701-17712.

Reimsnider, S., Manfredsson, F. P., Muzyczka, N., & Mandel, R. J. (2007). Time course of transgene expression after intrastriatal pseudotyped rAAV2/1, rAAV2/2, rAAV2/5, and rAAV2/8 transduction in the rat. Molecular Therapy, 15(8), 1504-1511.

Robertson, C. E., Ratai, E. M., & Kanwisher, N. (2016). Reduced GABAergic action in the autistic brain. *Current Biology*, *26*(1), 80-85.

Rosen, M. J., Sarro, E. C., Kelly, J. B., & Sanes, D. H. (2012). Diminished behavioral and neural sensitivity to sound modulation is associated with moderate developmental hearing loss. PLOS ONE 7(7): e41514.

Sale, A., Berardi, N., Spolidoro, M., Baroncelli, L., & Maffei, L. (2010). GABAergic inhibition in visual cortical plasticity. *Frontiers in cellular neuroscience*, 10.

Sanes, D. H., & Kotak, V. C. (2011). Developmental plasticity of auditory cortical inhibitory synapses. *Hearing research*, *279*(1-2), 140-148.

Sarro, E. C., & Sanes, D. H. (2011). The cost and benefit of juvenile training on adult perceptual skill. *Journal of Neuroscience*, *31*(14), 5383-5391.

Sarro, E. C., Kotak, V. C., Sanes, D. H., & Aoki, C. (2008). Hearing loss alters the subcellular distribution of presynaptic GAD and postsynaptic GABAA receptors in the auditory cortex. *Cerebral Cortex*, *18*(12), 2855-2867.

Shannon, R. V., Zeng, F. G., Kamath, V., Wygonski, J., & Ekelid, M. (1995). Speech recognition with primarily temporal cues. *Science*, *270*(5234), 303-304.

Singh, N. C., & Theunissen, F. E. (2003). Modulation spectra of natural sounds and ethological theories of auditory processing. The Journal of the Acoustical Society of America, 114(6), 3394-3411.

Szymczak, A. L., & Vignali, D. A. (2005). Development of 2A peptide-based strategies in the design of multicistronic vectors. *Expert opinion on biological therapy*, *5*(5), 627-638.

Takesian, A. E., & Hensch, T. K. (2013). Balancing plasticity/stability across brain development. *Progress in brain research*, *207*, 3-34.

668 Takesian, A. E., Kotak, V. C., & Sanes, D. H. (2012). Age-dependent effect of hearing loss on
669 cortical inhibitory synapse function. *Journal of neurophysiology*, *107*(3), 937-947.
670 Tamás, G., Simon, A. L. A., & Szabadics, J. (2003). Identified sources and targets of slow
671 inhibition in the neocortex. Science, 299(5614), 1902-1905.
672 Tao, W., Higgs, M. H., Spain, W. J., & Ransom, C. B. (2013). Postsynaptic GABAB receptors
673 enhance extrasynaptic GABAA receptor function in dentate gyrus granule cells. *Journal of*
674 *Neuroscience*, *33*(9), 3738-3743.
675 Turrigiano, G. G., & Nelson, S. B. (2004). Homeostatic plasticity in the developing nervous
676 system. Nature reviews neuroscience, 5(2), 97-107.
677 Vickers, E. D., Clark, C., Osypenko, D., Fratzl, A., Kochubey, O., Bettler, B., & Schneggenburger,
678 R. (2018). Parvalbumin-interneuron output synapses show spike-timing-dependent plasticity that
679 contributes to auditory map remodeling. *Neuron*, *99*(4), 720-735.
680 Vigot, R., Barbieri, S., Bräuner-Osborne, H., Turecek, R., Shigemoto, R., Zhang, Y. P., ... &
681 Bettler, B. (2006). Differential compartmentalization and distinct functions of GABAB receptor
682 variants. *Neuron*, *50*(4), 589-601.
683 von Trapp, G., Aloni, I., Young, S., Semple, M. N., & Sanes, D. H. (2017). Developmental hearing
684 loss impedes auditory task learning and performance in gerbils. *Hearing research*, *347*, 3-10.
685 Wang, L., & Maffei, A. (2014). Inhibitory plasticity dictates the sign of plasticity at excitatory
686 synapses. *Journal of Neuroscience*, *34*(4), 1083-1093.
687 Wehr, M., & Zador, A. M. (2003). Balanced inhibition underlies tuning and sharpens spike timing
688 in auditory cortex. *Nature*, *426*(6965), 442-446.
689 Wen, Y., Dong, Z., Liu, J., Axerio-Cilies, P., Du, Y., Li, J., … & Wang, Y. T. (2022). Glutamate and
690 GABAA receptor crosstalk mediates homeostatic regulation of neuronal excitation in the
691 mammalian brain. Signal Transduction and Targeted Therapy, 7(1), 1-18.
692 Wichmann, F. A., & Hill, N. J. (2001). The psychometric function: I. Fitting, sampling, and
693 goodness of fit. *Perception & psychophysics*, *63*(8), 1293-1313.
694 Wichmann, F. A., & Hill, N. J. (2001). The psychometric function: II. Bootstrap-based confidence
695 intervals and sampling. *Perception & psychophysics*, *63*(8), 1314-1329.
696 Yao, J. D., & Sanes, D. H. (2018). Developmental deprivation-induced perceptual and cortical
697 processing deficits in awake-behaving animals. *Elife*, *7*, e33891.
698 Yao, J. D., & Sanes, D. H. (2018). Developmental deprivation-induced perceptual and cortical
699 processing deficits in awake-behaving animals. *Elife*, *7*, e33891.
700 Zeng, F. G., Nie, K., Stickney, G. S., Kong, Y. Y., Vongphoe, M., Bhargave, A., ... & Cao, K.
701 (2005). Speech recognition with amplitude and frequency modulations. *Proceedings of the*
702 *National Academy of Sciences*, *102*(7), 2293-2298.
703 Zhang, L. I., Bao, S., & Merzenich, M. M. (2001). Persistent and specific influences of early
704 acoustic environments on primary auditory cortex. *Nature neuroscience*, *4*(11), 1123-1130.
705 Zorio, D. A., Monsma, S., Sanes, D. H., Golding, N. L., Rubel, E. W., & Wang, Y. (2019). De novo
706 sequencing and initial annotation of the Mongolian gerbil (Meriones unguiculatus) genome.
707 *Genomics*, *111*(3), 441-449.
708 Zufferey, R., Donello, J. E., Trono, D., & Hope, T. J. (1999). Woodchuck hepatitis virus
709 posttranscriptional regulatory element enhances expression of transgenes delivered by retroviral
710 vectors. *Journal of virology*, *73*(4), 2886-2892.

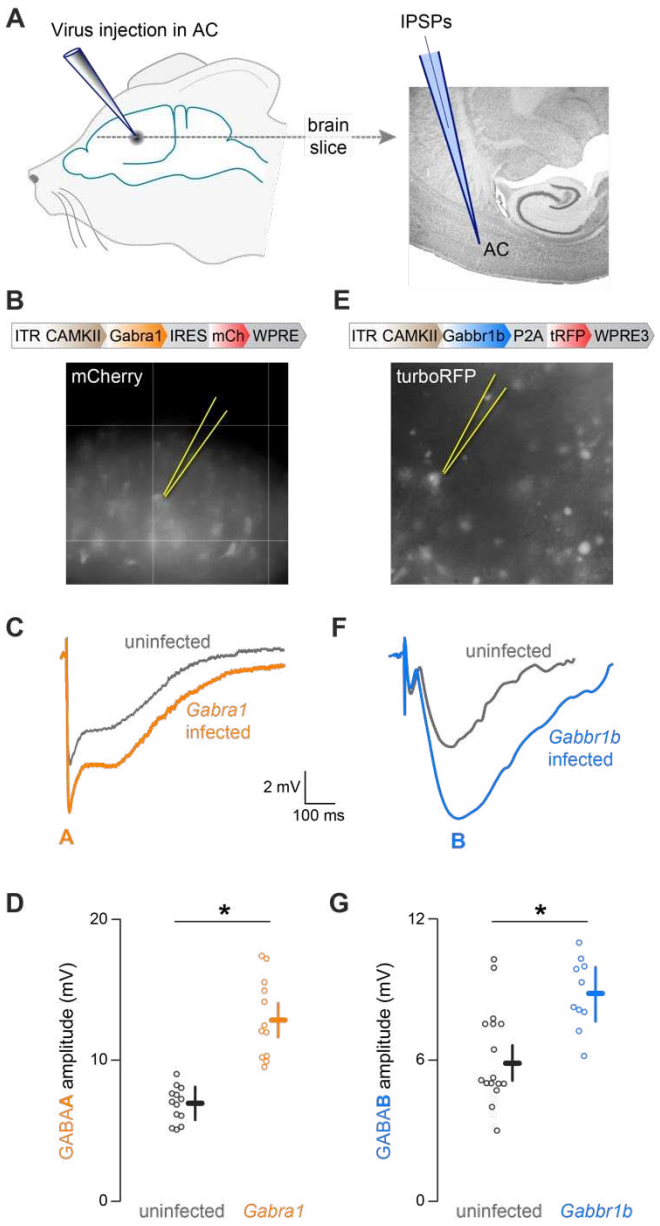

Figure 1: Viral vector design and validation. (A) For both Gabra1 and Gabbr1b AAVs, primary auditory cortex layer 2/3 was injected (Nanoject 2; Drummond) with approximately 250 nl of virus. After three weeks of expression a thalamocortical slice preparation was made and whole cell recordings (current clamp) from ACx L2/3 pyramidal cells were carried out. (B) Top, Diagram showing Gabra1 vector. Bottom, micrograph from ACx L2/3 showing Gabra1 infected cells (fluorescing, mCh) and one patched pyramidal neuron. (C) Representative evoked IPSP showing the larger GABAA potential in the Gabra1 infected pyramidal neuron (fluorescing patched cell from B) vs local uninfected (non-fluorescing) pyramidal neuron from the same slice. D) Plot diagram showing the average difference in $GABA_A$ IPSP amplitudes for uninfected versus Gabra1 infected pyramidal neurons. (E) Top, Diagram showing Gabbr1b vector. Bottom, micrograph from ACx L2/3 showing Gabbr1b infected cells (fluorescent, mCh) and one patched pyramidal neuron. (F) Representative evoked IPSP showing the larger $GABA_B$ potential in the Gabbr1b infected pyramidal neuron (fluorescing patched cell from C) vs local uninfected (non-fluorescing) pyramidal neuron from the same slice. (G) Plot diagram showing the average difference in $GABA_B$ IPSP amplitudes for uninfected versus Gabbr1b infected pyramidal neurons.

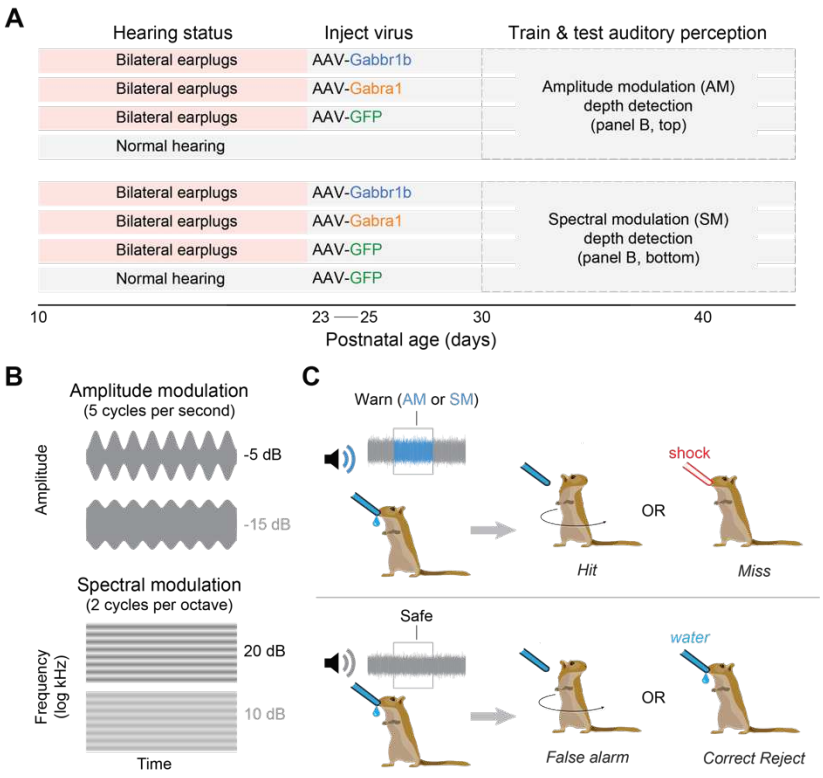

Figure 2: Experimental paradigm. (A) The experimental timeline, and each of the experimental groups is shown. (B) Example stimulus waveforms are shown for the AM depth detection task (top) and the SM depth detection task (bottom). (C) The Go-Nogo paradigm used for psychometric testing is shown.

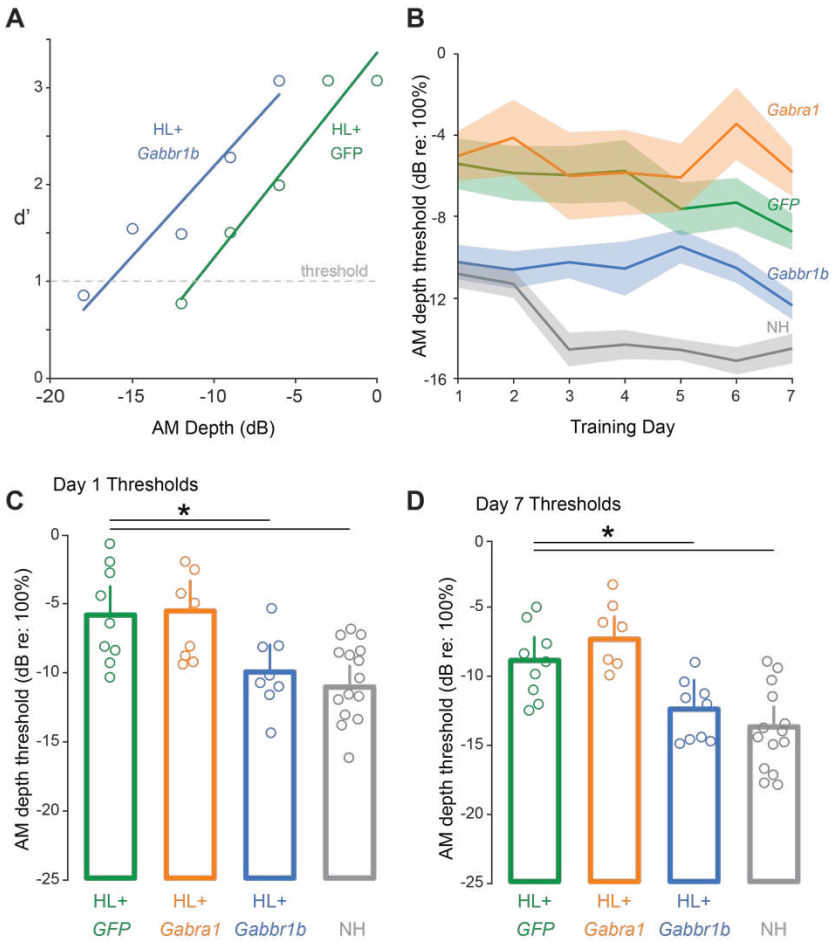

731 **Figure 3: Gabbr1b expression restores AM detection.** (A) Representative behavior for a HL-
732 reared gerbil expressing *Gabbr1b* (HL+*Gabbr1b*) and a HL-reared gerbil expressing *GFP*
733 (HL+*GFP*) in AC, both tested after transient hearing loss (HL). (B) AM depth thresholds achieved
734 by each group over training days. Mean ± SEM. (C) *Gabbr1b* expression in AC rescued AM
735 perception relative to *GFP* expression on day 1 of psychometric testing. Bars indicate significant
736 differences (see text for statistical values). (D) *Gabbr1b* expression in AC rescued AM perception
737 relative to *GFP* expression on day 7 of psychometric testing. Bars indicate significant differences
738 (see text for statistical values).

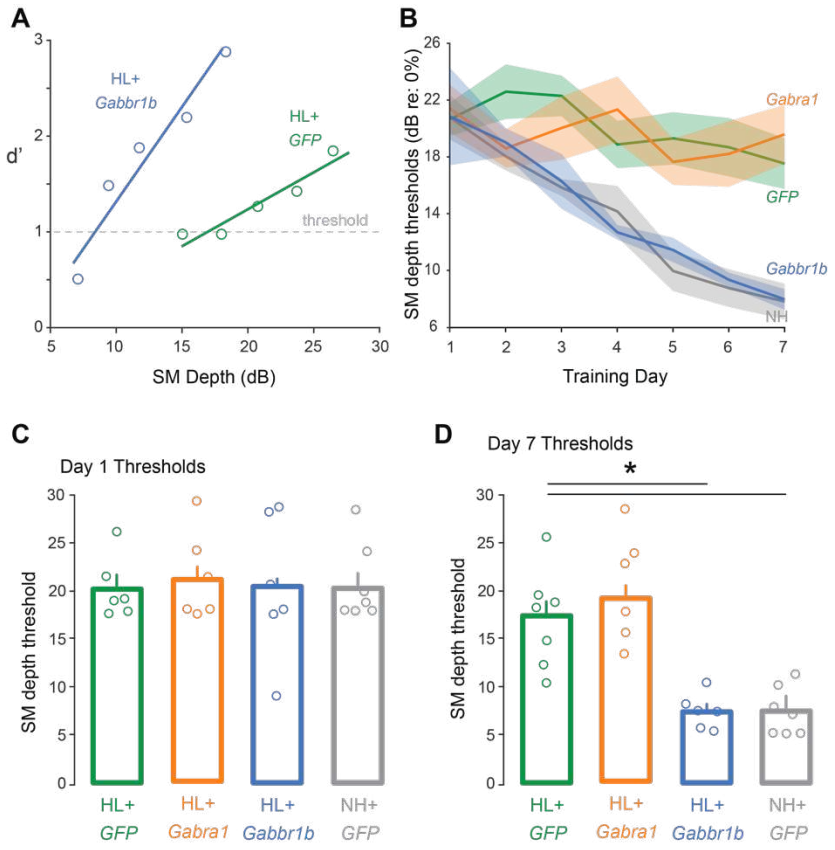

Figure 4: Gabbr1b expression restores SM detection. (A) Example psychometric curves of individual gerbils showing d' at each of the 5 modulation depths presented in a single session. The leftward shift of the HL+*Gabbr1b* function, relative to HL+*GFP* function indicates improved performance. Bars indicate significant differences (see text for statistical values). (B) Group performance on each day of psychometric testing. (C) There are no differences in SM modulation thresholds on the first day of psychometric testing, as calculated by fit crossing d' = 1. (D) SM thresholds on day 7 of psychometric testing. Both HL+*Gabbr1b* and NH+*GFP* groups performed significantly better than HL+*GFP* animals. Bars indicate significant differences (see text for statistical values).

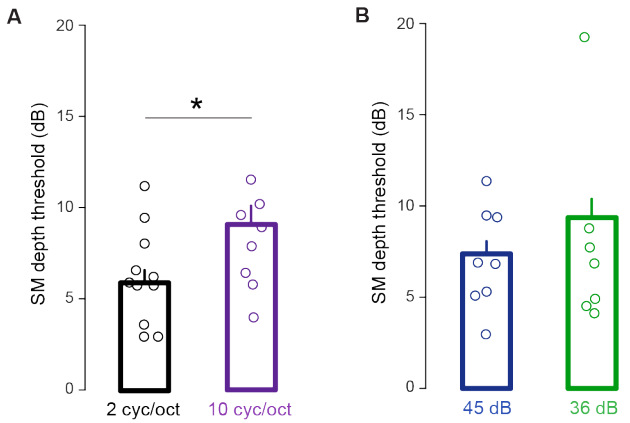

Supplemental Figure 1: Spectral modulation detection in normal hearing juvenile gerbils (A) NH animals display better thresholds for SM at 2 cycles/octave relative to 10. Bar indicates significant difference (see text for statistical value). (B) SM detection thresholds do not change significantly when sound is presented at a lower level of 36 dB SPL ($p = 0.593$).

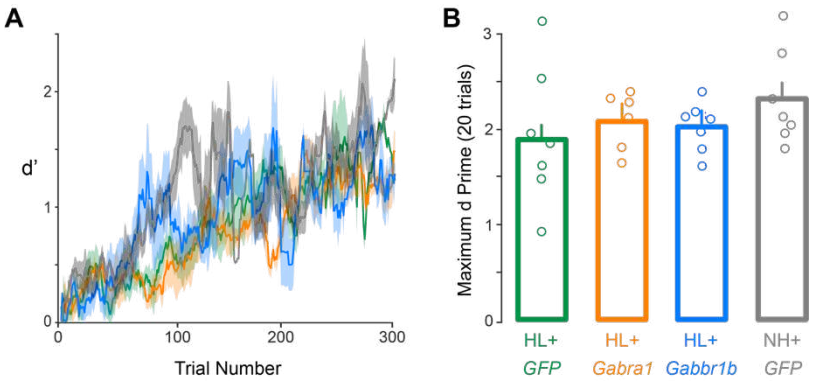

752 **Supplemental Figure 2: Procedural training for spectral modulation detection (**A) There
753 are no group differences in the number of trials required for procedural training (mean ± SEM,
754 moving window of 20 trials). (B) There are no significant differences in maximum d' achieved
755 during all procedural training over 20 trial windows (see text for statistical value).